

- Granulite Terrain of India, with implications for Gondwana studies. *Tectonics*, 2004, **23**; <http://dx.doi.org/10.1029/2002-TC001444>.
4. Tomson, J. K., Bhaskar Rao, Y. J., Vijaya Kumar, T. and Choudhary, A. K., Geochemistry and neodymium model ages of Precambrian charnockites, Southern Granulite Terrain, India: constraints on terrane assembly. *Precamb. Res.*, 2013, **227**, 295–315.
 5. Ramakrishnan, M. and Vaidyanathan, R., *Geology of India*, Geological Society of India, Bangalore, 2008, pp. 1–446.
 6. Ramakrishnan, M., *The Evolution of Pandyan Mobile Belt* (ed. Venkatachalapathy), Research Publishers, Singapore, 2013, pp. 1–40.
 7. Campanile, D., Nambiar, C. G., Bishop, P., Widdowson, M. and Brown, R., Sedimentation record in the Konkan–Kerala basin: implications for the evolution of the Western Ghats and the Western Indian passive margin. *Basin Res.*, 2008, **20**, 3–22.
 8. Radhakrishna, T., Dallmeyer, R. D. and Joseph, M., Palaeomagnetism and $^{36}\text{Ar}/^{40}\text{Ar}$ vs $^{39}\text{Ar}/^{40}\text{Ar}$ isotope correlation ages of dyke swarms in central Kerala, India: tectonic implications. *Earth Planet. Sci. Lett.*, 1994, **121**, 213–226.
 9. Mahadevan, T. M., A unitary model of evolution of the Precambrian Indian shield. Int. Sympo. Charnockite and granulite facies rocks. *Geol. Assoc. Tamil Nadu*, 1999, 153–174.
 10. Mahadevan, T. M., Kuppam–Palani transect programme and new insights into continental evolution. *Mem. Geol. Surv. India*, 2003, **53**, 99–114.
 11. Plavska, D., Collins, A. S., Foden, J. F., Kropinski, L., Santosh, M., Chetty, T. R. K. and Clark, C., Delineating crustal domains in Peninsular India: age and chemistry of orthopyroxene-bearing felsic gneisses in the Madurai Block. *Precamb. Res.*, 2012, 198–199, 77–93.
 12. Radhakrishna, T., Maluski, H., Mitchell, J. G. and Joseph, M., $^{40}\text{Ar}/^{39}\text{Ar}$ and K/Ar geochronology of the dykes from the south Indian granulite terrain. *Tectonophysics*, 1999, **304**, 109–129.
 13. Geological Survey of India (GSI), Geological map of Kerala and Tamil Nadu, 1995.
 14. Soman, K., *Geology of Kerala*, Geological Society of India, Bangalore, 2002, pp. 1–335.
 15. Project Vasundhara: Generalised Geological Map (scale 1 : 2 million), Geological Survey of India and Indian Space Research Organization, Bangalore, 1994.
 16. Narula, P. L., Acharyya, S. K. and Banerjee, J. (eds), *Seismotectonic Atlas of the Indian Subcontinent and Adjoining Areas*, Geological Survey of India, 2000, Special Publication Series 59.
 17. Harikumar, P., Rajaram, M. and Balakrishnan, T. S., Aeromagnetic study of Peninsular India. *Proc. Indian Acad. Sci. (Earth Planet Sci.)*, 2000, **109**(3), 381–391.
 18. Rajaram, M. and Anand, S. P., Crustal structure of South India from aeromagnetic data. *J. Virtual Exp.*, 2003, **12**, 72–82.
 19. Radhakrishna, M., Verma, R. K. and Purushotham, A. K., Lithospheric structure below the eastern Arabian Sea and adjoining West Coast of India based on integrated analysis of gravity and seismic data. *Mar. Geophys. Res.*, 2002, **23**, 25–42.
 20. Bhaskar Rao, Y. J., Janardhan, A. S., Vijaya Kumar, T., Narayana, B. L., Dayal, A. M., Taylor, P. N. and Chetty, T. R. K., Sm–Nd model ages and Rb–Sr isotopic systematics of charnockite gneisses across the Cauvery shear zone, south India, implication for Archean, Neoproterozoic terrane boundary in the Granulite Terrain. *Tectonics of the Southern Granulite Terrain, Kuppam–Palani Geotranssect* (ed. Ramkrishnan, M.), Geological Society of India Memoir, 2003, **50**, 297–317.
 21. Brandt, B., Raith, M. M., Schenk, V., Sengupta, P., Srikantappa, C. and Gerdes, A., Crustal evolution of the Southern Granulite Terrane, south India: new geochronological and geochemical data for felsic orthogneisses and granites. *Precamb. Res.*, 2014, **246**, 91–122.
 22. Radhakrishna, T. and Joseph, M., Geochemistry and paleomagnetism of Late Cretaceous mafic dikes in Kerala, southwest coast of India in relation to large igneous provinces and mantle plumes in the Indian Ocean region. *Geol. Soc. Am. Bull.*, 2012, **124**(1/2), 240–255.
 23. Elizabeth, J., Catlos, Chandra, S. Dubey and Poovalingam Sivasubramanian, Monazite ages from carbonatites and high-grade assemblages along the Kambam Fault (Southern Granulite Terrane, South India). *Am. Mineral.*, 2008, **93**(8–9), 1230–1244.
 24. Saikia, U., Rai, S. S., Subrahmanyam, M., Satyajit Dutta, Somasish Bose, Borah, K. and Meena, R., Accurate location and focal mechanism of small earthquakes near Idukki Reservoir, Kerala: implication for earthquake genesis. *Curr. Sci.*, 2014, **107**(11), 1885–1891.
 25. Rajendran, C. P., John, B., Sreekumari, K. and Rajendran, K., Re-assessing the Earthquake Hazard in Kerala based on the historical and current seismicity. *J. Geol. Soc. India*, 2009, **73**, 785–802.
 26. Brandt, S., Schenk, V., Raith, M. M., Appel, P., Gerdes, A. and Srikantappa, C., Late Neoproterozoic P–T evolution of HP-UHT Granulites from the Palani Hills (South India): New Constraints from Phase Diagram Modelling, LA-ICP-MS Zircon Dating and in-situ EMP Monazite Dating. *J. Petrol.*, 2011, **52**(9), 1813–1856.
- ACKNOWLEDGEMENTS. We are grateful to Prof. Mita Rajaram and Dr S. P. Anand, Indian Institute of Geomagnetism (IIG), Mumbai, for sparing aeromagnetic maps cited in this paper. We thank Dr M. Ramakrishnan, Dr S. Sinha Roy and Dr T. Radhakrishna, for reviewing an earlier version of this paper. The valuable suggestions from the Editor and reviewers have helped to improve this paper considerably. We express our thanks to Dr K. Sajjan, Head, Department of Marine Geology and Geophysics, Cochin University of Science and Technology, Cochin, for permitting to make use of the facilities. The first author thank Dr S. Rajendran for guidance, Dr M. Radhakrishna, IIT–Bombay for sparing a part of the gravity data and guidance in the initial geophysical studies and Dr John Kurian, NCAOR, Goa and Dr P. S. Sunil, IIG, Mumbai, and Mr S. K. Arun, GSI, Mangalore, for helping in data acquisition.
- Received and accepted 19 July 2016
- doi: 10.18520/cs/v111/i11/1847-1853

Iron oxide–copper–gold-type mineralization in Machanur area, Eastern Dharwar Craton, India

Abhishek Kumar Shukla*, Parasuram Behera, K. Basavaraja and M. Mohanty

Geological Survey of India, Vasudha Bhavan, Kumarswamy Layout, Bengaluru 560 078, India

Parallel to the Krishna river course, a set of ENE to WSW trending brittle–ductile shear zones affecting the Neoproterozoic pink porphyritic granite remains athwart the NW–SE tectonic fabric of the Eastern Dharwar Craton (EDC) in Raichur and Gulbarga districts, Karnataka, India. These zones are not only manifested by intense mylonitization, brecciation and fracturing, but also witness several episodes of mafic and felsic intrusions. At Machanur, Raichur district a 5 km long and 400 m wide shear zone hosts copper,

*For correspondence. (e-mail: abhishek.shukla@gsi.gov.in)

gold and REE mineralization both in specularite-rich hydrothermal veins and as disseminations within the dolerite dykes. The mineralization is associated with well-developed zones of hydrothermal alteration in the form of propylitization, carbonatization, epidotization and silicification with patches of strong iron-staining and fracture-filled iron solution dominantly in the footwall side. Due to similarity with many iron oxide–copper–gold-type deposits, this prospect in Machanur is interpreted as iron oxide–copper–gold-type mineralization.

Keywords: Brittle–ductile, hydrothermal alteration, ore deposits, mineralization, shear zones.

RELATIVELY recent categorizations of iron oxide–copper–gold (IOCG) ore deposits have attracted the attention of exploration geologists around the globe. Due to its polymetallic nature and huge resource, it has become an important class of economic deposits. The IOCG classes are globally characterized by high tonnage and low-grade ore, and vary in age, size, host rock, alteration associations, geochemical signature and physical properties. The giant and famous IOCG-class Olympic Dam deposit (Cu–Au–Ag–U–REE) discovered in 1975 in South Australia is the world's fourth largest Cu, fifth largest Au and the largest U deposit¹. In India, Cu–Au mineralization in Palaeoproterozoic Salumber–Ghatol belt, Aravalli Supergroup, Rajasthan²; Cu deposit (IOCG) at Thanewasna, Western Bastar Craton, Central India³, and Jaduguda U–(Cu–Fe) mineralization⁴ are considered as IOCG-type mineralization.

The Eastern Dharwar Craton (EDC) lying east of the Gadag–Mandya Shear Zone and the Closepet Granite is considered to represent the Dharwar batholith because of the prolific 2.5 Ga calc-alkaline granitic magmatism⁵. Several occurrences represent granitoid-hosted copper mineralization in the granite–greenstone terrains of EDC as Thinthini, Machanur, Malatgud Kallur, Gogalgatti and Yegavakota. The mineralization at these localities is mainly cavity-filling, epigenetic hydrothermal-type⁶. The Machanur mineralization in Raichur district, Karnataka, India is a promising base-metal prospect occurring within the mylonitized pink granite having intrusive relationship with the well-known Hutti–Maski schist belt⁷. The present communication reports Fe–Cu–Au mineralization in Machanur, possibly corresponding to the IOCG-type in EDC.

Regionally the area forms a part of the EDC consisting of granite greenstone ensemble of Dharwar Supergroup (2600–2800 Ma). These granites are represented by an older grey granite/granodiorite phase and younger pink porphyritic phase⁸. The latter phase is invariably identified with the 2.5 Ga Closepet type calc-alkaline granite. The other lithounits in the area comprise amphibolites, minor BIF and pillowed metabasalt occurring as dismembered enclaves of the greenstone belts. Later intrusives

include dolerite, gabbro, pegmatite and quartz veins. The prominent schist belts of the EDC well-known for their gold potential are Kolar, Ramagiri, Hutti, Kushtagi and Hungund⁹. The metavolcanic rocks of the schist belts are 2700 Ma old and are surrounded by 2700–2500 Ma granite and gneisses with a record of distinct geological histories¹⁰. The entire eastern block of the Dharwar Craton is believed to be an accreted terrane and the schist belts represent terrane boundaries. The contact between the schist belts and the gneisses is generally tectonic in nature. However, in the Hutti and Ramgiri schist belts, an intrusive relation between late phase granite and supracrustal rocks has been reported⁷. The present study area around Machanur, lying on the northern proximity of Hutti–Maski schist belt and along the NW–SE trending Krishna lineament comprises dominantly pink-coloured porphyritic granite being intruded by later felsic and mafic dykes (Figure 1 c).

Mineralization in the study area is confined to a prominent 400–500 m wide brittle–ductile shear zone trending ENE to WSW and extending for 5 km. Copper mineralization is confined in the 150–200 m wide central part of the shear zone. The foliation in mylonitized pink granite shows N70°E–S70°W trend with vertical to steep northerly dip. The shear zone exhibits a range of textures from incipient cracking, grading, brecciation and mylonite suggesting brittle–ductile nature of this zone. Within the shear zone minor variation in the dip amount, with constant trend suggest development of a flower structure.

Detailed geological map reveals (Figure 1 c) the presence of two discrete dolerite dykes. Due to the steep northerly dip of the shear zone, the northern dyke is termed as hanging wall dyke and the southern dyke as footwall dyke. The former is less deformed and altered having width ranging from 2 to 5 m. The latter has a width ranging from 15 to 25 m and has undergone extensive carbonate alteration, quartz carbonate veining and fracturing. Hence it is not certain whether these represent two separate dykes as marked in the map or could be one dyke separated on the margins of brittle–ductile shear zone. Due to low exposure density (15%–20%), correlation between various alteration zones becomes difficult. Although dissemination of pyrite–chalcopyrite is ubiquitous in the dolerite dyke, malachite stains associated with carbonate alteration along with epidote and calcite veins are more pronounced in the footwall dolerite dyke. The central part of the zone (100–200 m wide) witnessed extensive brecciation of the pink porphyritic granite and also intrusion of haematite/specularite veins containing sulphide minerals. Restricted areas within this zone contain S–C mylonite fabric, suggesting a dextral sense. Breccia displays a range of textures from incipient cracking, grading to matrix-dominated breccia, suggesting their development in a brittle–ductile regime.

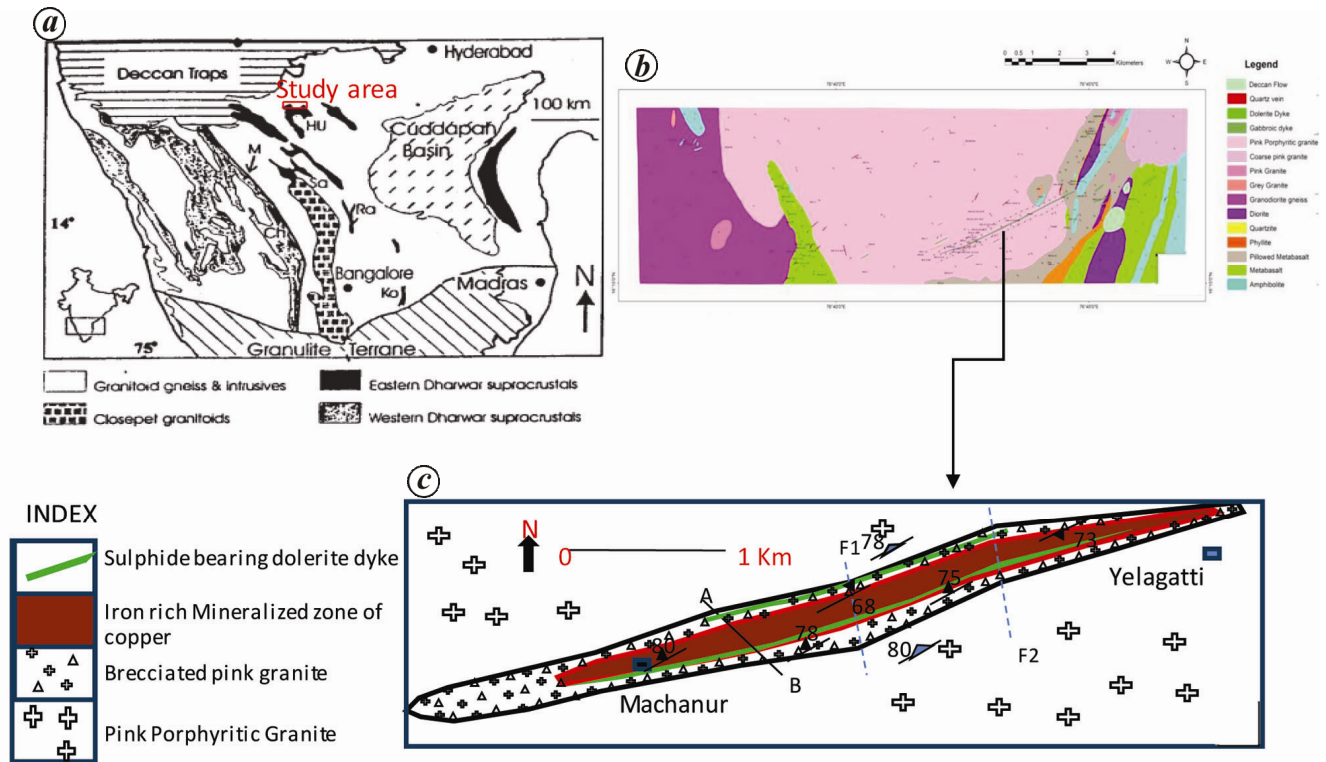


Figure 1. Location (a), geology (b), detailed mineralized (c) map of Machanur area, Raichur district, Karnataka, India.



Figure 2. Hand specimens of mineralized zone. a, Malachite stain within calcite vein. b, Malachite-rich quartz vein. c, Alternate specularite and calcite layers containing base metal sulphides.

Leached copper is present as malachite stains and encrustations confined to the shear planes and joints in quartz calcite veins (Figure 2 a and b). The other sulphide minerals present in minor amounts are sphalerite and galena (Figure 2 c) in the calcite veins. Dissemination and aggregates of chalcocopyrite constitute the major ore minerals of copper, especially in quartz sulphide and quartz–calcite veins. It also occurs as stringers, filling tiny fractures in the mylonites. Petrographic studies reveal that pyrite occurs in two generations, the earlier forming anhedral, fractured grains having corroded boundaries. Pyrite of younger generation occurs as fresh, euhedral crystals and is free from fractures. Chalcocopyrite occurs both as tiny inclusions within the chlorite and as

discrete grains within calcite-rich quartz veins (Figure 3 a). Often anhedral grains of native gold occur as floats within haematite (Figure 3 b). At several instances, chalcocopyrite confined to haematite is associated with rutile (Figure 3 d). Goethite and covellite are also developed along the margins of pyrite and chalcocopyrite (Figure 3 c).

Presence of intricately associated quartz and epidote veins cutting each other and fracture-filled iron hydroxide indicate hydrothermal fluid movement in successive stages. The oxide minerals present are haematite/specularite with minor magnetite. Specularite commonly occurs as fracture-filling veins within the shear zone, often forming an anastomosing network and as massive concentration or as parallel thin bands. Fracture-filled

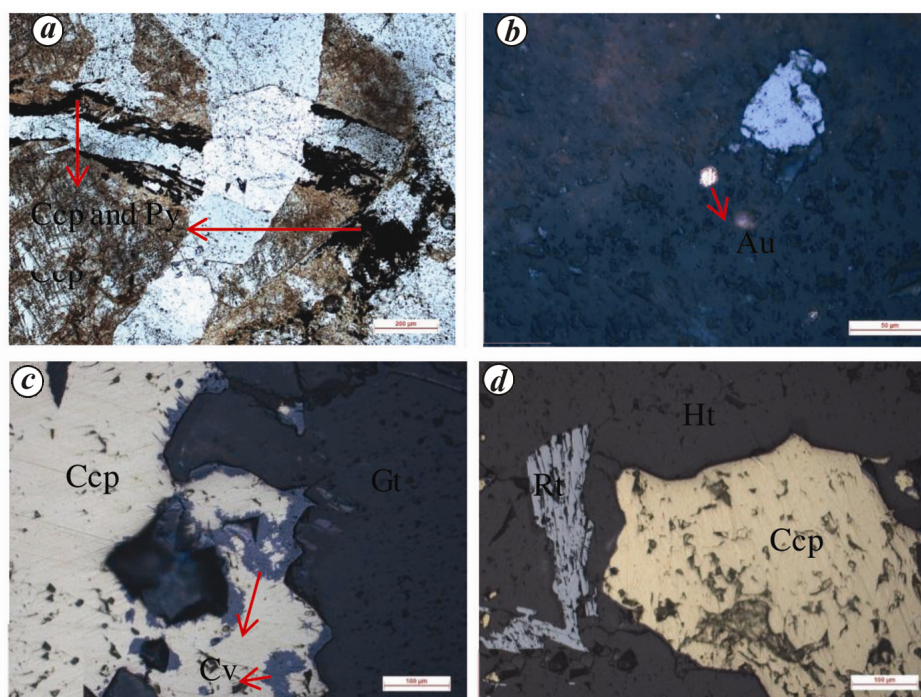


Figure 3. Photomicrographs of ore minerals and alteration patterns of Machanur IOCG mineralization. *a*, Multi-generation hydrothermal veinlets containing pyrite (Py)/chalcopyrite (Ccp) grains. *b*, Specularite/hematite (Ht) veins in fine matrix of granite breccia, the dominant carrier of base metal and gold (Au) minerals. *c*, Goethite (Gt) and covellite (Cv) developing along the margins of pyrite and chalcopyrite. *d*, Chalcopyrite confined to haematite in association with rutile (Rt).

specularite is also present in quartz veins and dolerite dyke, and is mostly associated with calcite vein. Magnetite is not common, but can be identified as isolated grains developed in calcite–quartz veins. Extensive silicification of pink porphyritic granite with replacement of silicate minerals and anastomosing quartz veining (with chalcopyrite and pyrite) containing brecciated granite clasts are noticeable.

Successive phases of alteration are deciphered as revealed by early-formed, albite-rich veins traversed and offset by later quartz–carbonate veins (Figure 3 *a*). The preliminary study reveals that basemetal and gold mineralization is post-sodic alteration as dissemination is dominantly contained in later haematite-rich veins (Figure 3 *b*).

Chloritization is extensive and at places it leads to destruction of original texture of the pink porphyritic granites. However, appearance of chlorite all along the mineralized zone is not of one generation. There are at least three generations of chlorite, the oldest phase being developed from the alteration of pyroxene/hornblende in the parent rock. The latter phase of chlorite is developed in late-stage fracture filling of quartz and calcite veins. Carbonate alteration appears to have become progressively greater as the style of alteration evolved from breccia matrix-type to vein-type. Calcite is also generally more abundant in the footwall side of the ore body, often partially replacing pre-existing K-feldspar of the granite.

Carbonate veins (calcite/ankerite) cut across the specularite breccia, indicating that they have formed later in the hydrothermal system. Very fine cracks filled with haematite, biotite and epidote are interpreted to belong to this stage and are recorded up to several kilometres away from the main zone. Cross-cutting relationship of veinlets observed in the marginal part of the shear zone suggests that chlorite–epidote–quartz phase postdates K-feldspar/albite alteration. The distal K–Fe–Mg and proximal feldspathized carbonate alteration are not well-pronounced in this area².

Signature of intense hydrothermal activity is recorded by a set of alteration zones all along the 5 km strike and 400–500 m width of the shear zone. The alteration system evolved through a series of distinct stages, causing a series of overprints that produced complex mineralogical patterns. A classification of alteration and veining products in their order of development is as follows: (1) sodic and/or potassic alteration; (2) ferruginization, propylitic and sericitization spatially associated with the mineralization; (3) carbonatization, and (4) fracturing and quartz calcite veining.

The earliest alteration produced sodic and sodic–potassic assemblages are broadly similar to those that characterize regionally extensive alteration systems in the exposed Neoproterozoic pink porphyritic granite. The timing of this broad alteration pattern is prior to the shearing in Machanur area and is possibly linked to syenite/

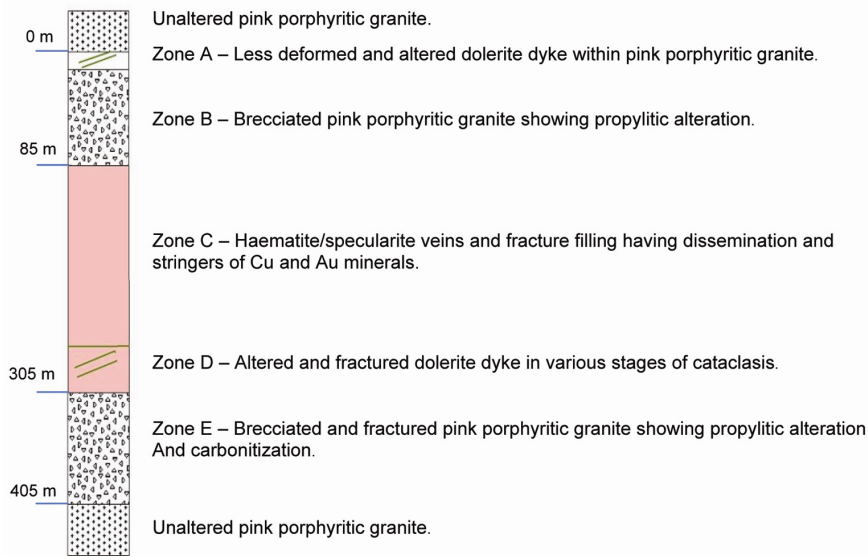


Figure 4. Litholog along line *AB* (in Figure 1) of Machanur IOCG mineralization.

Table 1. Descriptive analysis of alteration zone characterizing basic differences in each zone as noted in the litholog (Figure 4)

Description	Zone A	Zone B	Zone C	Zone D	Zone E
Width (m)	2–5	80	200	15–25	100
Host rock	Dolerite dyke	Brecciated pink granite	Mylonitized pink granite	Dolerite dyke	Brecciated pink granite
Carbonatization	Less	Absent	High	Very high	Less
Silicification	Very less	High	Very high	Less	High
Malachite stain	Absent	Very less	Very high	Very high	Less
Chloritization	Less	Very less	High	Very high	High
Feruginization	Absent	Less	Very high	Less	High
Sulphide mineral	Very less	Less	Very high	High	Absent
Oxide mineral	Absent	Less	Very high	High	Less

alkaline magmatism post-Closepet granite (2.5 Ga) intrusion. This apparently affected rocks throughout the area although later events, especially in the vicinity of the shear zone, were too strong to have preserved the potassic minerals. K-metasomatized rocks contain orthoclase–chlorite–epidote with minor quartz and haematite assemblages. This stage is superimposed by texturally pervasive and destructive replacement of the host rock by albite-rich veins and breccia zones containing various combinations of fluorite and sericite.

Figure 4 provides a description of alteration and litholog across the strike of shear zone along line *AB* in Figure 1 *c*. Table 1 provides details of all alteration zones. Zone A – Carbonatization resulting in parallel to anastomosing calcite and epidote veins in the deformed dolerite dyke. The dimension of these veins widely varies from a few millimetres to 10 cm. The width of this dyke ranges from 2 to 5 m. However, overall percentage of carbonitization is less compared to zone D. The deformed dolerite dyke of this zone has disseminated sulphides. Zone B – It is characterized by propylitic alteration in brecciated pink granite resulting in the development of chlorite and epidote possibly derived from hornblende and biotite. The foliation in sheared pink granite shows

ENE–WSW trend with vertical to steep northerly dip. In this zone, feldspar in the brecciated pink porphyritic granite is usually dull with development of epidote, chlorite, albite and calcite, indicating medium to low temperature of formation. Zone C – It is mainly specularite-rich Cu-mineralized zone having mineral assemblage of quartz + haematite + siderite + calcite + epidote within the mylonitized pink porphyritic granite. The zone has witnessed extensive silicification with ramifying thin chert veins having profuse malachite stains. At places, the specularite/haematite bands occur as alternate bandings with silica resulting in the appearance of a banded rock. Sulphide minerals as chalcopyrite, pyrite and bornite are common in this zone. The width of this zone is around 200 m. Percentage of malachite alteration is highest in this zone compared to the rest. Zone D – This zone is characterized by highly fractured, carbonated, epidotized, dolerite dyke intruded within mineralized zone containing chalcopyrite, pyrite, covelite and bornite. Width of this dolerite dyke varies from 15 to 25 m. Percentage of carbonatization resulting in parallel to anastomosing calcite veins is more in this zone compared to rest of alteration zones. Zone E – This zone is characterized by propylitic alteration in brecciated pink porphyritic granite at the

footwall side. Apart from the mineral assemblage like epidote–chlorite–albite and calcite, iron oxide and hydroxides have filled the fracture planes. It invariably contains disseminated pyrite. This is caused by extensive fracturing and jointing in the country rock permitting easy access of hydrothermal solutions. Often boudins of calcite stand out in the country rock along the mylonitic foliation. Here K-feldspar is less altered and zone-E has undergone intense fracturing and jointing compared to zone B.

At Machanur selected grab and trench samples collected systematically across the mineralized/alteration zone suggest a distinct and geochemically diverse pattern of minor elements, including LREE. The analysis of base metals and trace elements, including Au was carried out by Flame-AAS/GTA-AAS method at GSI Chemical Laboratory, Bengaluru with error factor of 2%. The REE and U were analysed in GSI Chemical Laboratory, Hyderabad employing ICP-MS. Most of the analytical results (28 nos.) yield average 0.24% of Cu, with maximum value of 5.2% Cu, average 75 ppm REE with 62 ppm LREE and 130 ppb Au. The average U content in the mineralized zone is 1.69 ppm ($n = 25$ nos) with maximum 3.75 ppm and minimum 0.44 ppm. The haematite-rich portions show average 13.5% Fe with <1 wt % TiO₂. Cu/Fe values of Machanur (1/30) are well within the prescribed limit of many world-class IOCG deposits¹ (Cu/Fe ~1/15 to 1/30).

The alteration system evolved in the Machanur prospect is similar to the Ernest Henry – a Proterozoic magnetite-dominated deposit in Australia, with a difference that the former is haematite-dominated. As in the case of Ernest Henry deposit, here also alteration has developed through a series of distinct stages, causing a series of overprints that produced complex mineralogical patterns¹. Since hydrothermal alteration in the structurally controlled mineralized zone is one of the key features of IOCG type of deposits, the Machanur mineralization displays the following features to be categorized as IOCG-type: (i) presence of Cu as economic mineral with traces of gold; (ii) hydrothermal vein, breccia, fracture filling, vug and comb structure, characteristically in brittle–ductile shear zone; (iii) abundant haematite/specularite with minor magnetite, and (iv) common association with large-scale carbonate alteration and development of a set of hydrothermal alteration zones all along and across the shear zone.

Critical issues in IOCG genesis are topics of ongoing debate concerning the source of metals, ore fluids and other vital components of the ore-forming systems, such as Cl and S. Proper documentation of field observations, geologic characteristics of IOCG deposits and their causative hydrothermal systems may help in a better understanding of its genesis. In the present case the base metal and gold mineralization is dominant associated with Fe-dominant hydrothermal fluid. There is domi-

nance of carbonic fluid over the quartz veins. Various genetic models have been proposed for IOCG deposits that can be broadly divided into those involving magmatic and non-magmatic fluid source¹¹. In the case of Machanur mineralization magmatic fluid source is ruled out as intense hydrothermal activity has been noted which is characteristic of non-magmatic fluid source. Although to find the specific genetic model of Machanur IOCG mineralization, detailed laboratory studies are essential, based on geological features observed in the field, alteration assemblage and pattern of its evolution and mineralogical association Machanur base metal and gold mineralization can be ascribed to the IOCG type, as reported here.

- Williams, P. J. *et al.*, *Iron Oxide Copper–Gold Deposits: Geology, Space-Time Distribution, and Possible Modes of Origin*, Society of Economic Geologists, Inc. Economic Geology 100th Anniversary Volume, 2005, pp. 371–405.
- Fareeduddin, I. R. K. and Chander, S., Petrology, geochemistry and fluid inclusion studies of Cu–Au mineralization in paleoproterozoic Salumber–Ghatol Belt, Aravalli Supergroup, Rajasthan. *J. Geol. Soc. India*, 2012, **80**, 5–38.
- Dora, M. L., Saha, A. K., Randive, K. R. and Rao, K. K., Geological framework and general characteristics of Cu deposit (IOCG) at Thanewasna, Western Bastar craton, Central India. In 34th International Geological Congress, Brisbane, Australia, 5–10 August 2012.
- Pal, D. C., Trumbull, R. B. and Wiedenbeck, M., Chemical and boron isotope compositions of tourmaline from the Jaduguda U (–Cu–Fe) deposit, Singhbhum shear zone, India: implications for the source and evolution of the mineralizing fluid. *Chem. Geol.*, 2010, **277**(3–4), 245–260.
- Rogers, A. J., Kolb, J., Meyer, F. M. and Armstrong, R. A., Tectono-magmatic evolution of the Hutti-Maski Greenstone Belt, India: Constrained using geochemical and geochronological data. *J. Asian Earth Sci.*, 2007, **31**, 55–70.
- Radhakrishna, B. P., Mineralization episodes in the Dharwar craton of peninsular India. *J. Geol. Soc. India*, 1976, **17**, 79–88.
- Srikantia, S. V., Geology of Hutti-Maski greenstone belt. The Hutti Gold Mines Company Limited, Golden Jubilee Souvenir 1948–1998, pp. 23–33.
- Swaminath, J., Ramakrishnan, M. and Viswanatha, M. N., Dharwar stratigraphic model and Karnataka craton evolution. *Rec. Geol. Surv. India*, 1976, **107**, 149–175.
- Curtis, L. C. and Radhakrishna, B. P., Hutti Gold Mine: Into the 21st Century: Bangalore, Economic Geology Series 5, Geological Society of India, 1995, p. 176.
- Balakrishnan, S., Rajamani, V. and Hanson, G., U–Pb ages for zircon and titanites from the Ramagiri area, southern India: evidence for the accretionary origin of Eastern Dharwar craton during the late Archaean. *J. Geol. Soc. India*, 1999, **107**, 69–86.
- Barton, M. D. and Johnson, D. A., Evaporitic-source model for igneous related Fe oxide – (REE–Cu–Au–U) mineralization. *Econ. Geol.*, 1996, **24**, 259–262.

ACKNOWLEDGEMENTS. We thank C. G. Hemantha Kumar (GSI, Bengaluru) for help and guidance and Dr Mohamed Shareef (GSI, Bengaluru) for help in petrographic studies.

Received 31 March 2016; revised accepted 1 August 2016

doi: 10.18520/cs/v111/i11/1853-1858